ACS APPLIED MATERIALS & INTERFACES

Research Article

www.acsami.org

# Self-Powered Humidity Sensor Based on Graphene Oxide Composite Film Intercalated by Poly(Sodium 4-Styrenesulfonate)

Hyun-Woo Yu,[†] Hyoung Kyu Kim,[‡] Taewoo Kim,[§] Kyoung Min Bae,[†] Sung Min Seo,[∥] Jong-Man Kim,[†,‡] Tae June Kang,*[,†,‡] and Yong Hyup Kim*[,§]

[†]Department of Nanofusion Technology, Pusan National University, 30 Jangjeon-dong, Geumjung-gu, Busan 609-735, South Korea

[‡]Department of Nanomechatronics Engineering, Pusan National University, 30 Jangjeon-dong, Geumjung-gu, Busan 609-735, South Korea

[§]School of Mechanical and Aerospace Engineering, Seoul National University, 1 Gwanak-ro, Gwanak-gu, Seoul 151-742, South Korea

[∥]DRAM Design Team, Memory Division, Samsung Electronics, Hwasung-City, Gyeonggi-do, South Korea

Supporting Information

**ABSTRACT:** This Research Article reports self-powered humidity sensors based on graphene oxide (GO) and poly(sodium 4-styrenesulfonate) (PSS)-intercalated GO composite films used as the humidity-responsive dielectrics. A hydrophilic and electrically-insulating PSS polymer was used as an intercalant between the individual GO platelets to enhance the water permeation characteristics. Capacitive-type humidity sensors fabricated by forming metal electrodes on both sides of the GO and GO-PSS films were installed into the charge pumping system, which can produce a voltage output as a response to humidity sensing. While both sensors based on GO and GO-PSS dielectrics responded stably and reversibly to the changes in RH, the GO-PSS sensor showed enhanced sensing responses compared to the GO sensor, providing ~5.6 times higher voltage output and 3 times faster responses in humidity sensing.

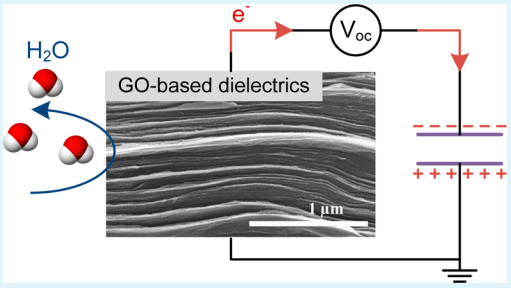


**KEYWORDS:** *graphene oxide, poly(sodium 4-styrenesulfonate), humidity sensor, dielectric*

## INTRODUCTION

Humidity sensors are of great demand in industry and environmental fields.[1] Considerable efforts have been made to develop humidity sensors based on various transduction principles, such as capacitive,[2,3] resistive,[4,5] acoustic,[6,7] and optical[8,9] detection. To further improve the sensing performance in terms of the sensitivity, selectivity and response time,[10−12] nanoscale materials have been investigated as humidity-responsive materials. Among these nanomaterials, graphene oxide (GO) thin films have attracted considerable attention because of their strong interaction between water molecules and oxygen functional groups on the surface.[13−15]

Graphene oxide film is a laminated material consisting of oxygenated graphene platelets.[16,17] Graphene oxide contains a wide range of oxygen functional groups, such as hydroxyl and epoxy groups on the basal plane and carboxylic acid groups at the edges,[16] which render the GO film hydrophilic. In conjunction with the hydrophilic property that contributes to water adsorption on the film, the layered and interlocked structure of the GO film effectively undergoes the permeation of water molecules into the film under humid conditions.[13,14] Nanoscale capillaries between individual GO platelets generate low-friction flow of water molecules on the graphene surface, hence the permeation process appears to be quite fast and reversible.[17] As a result of water permeation, the interlayer distance between the GO platelets varies reversibly from 6 to 12 Å depending on the relative humidity (RH);[13,15] the interlayer distance increases with increasing RH. This suggests that GO films can be used to monitor the humidity in the environment by characterizing the changes in the physical properties of the film. For example, the mass change of the GO film caused by the adsorption/desorption of water molecules was monitored using a quartz crystal microbalance (QCM).[18] Analogous to a classical bimorph structure, the character of large volume expansion in a water-swollen GO film was used to develop stress-based humidity sensors by coating a thin GO film on the flexible microstructure.[19]

The electrical perturbations in the GO film caused by electrical interactions between water molecules and GO platelets have come to the fore for the real-time, electrical detection of humidity. In particular, the water molecules that are hydrogen-bonded to oxygen groups on the GO surface easily lose a degree of rotational freedom as a consequence of the strong interactions in the layered and interlocked structure.[20] This confined water interaction leads to an increase in dielectric strength across the hydrated GO layers and a decrease in the electrical conductivity of the film.[20−22] Motivated by the unique changes in the electrical properties,

Received: February 24, 2014
Accepted: May 12, 2014
Published: May 12, 2014

   dx.doi.org/10.1021/am501151v | ACS Appl. Mater. Interfaces 2014, 6, 8320−8326

resistive-type humidity sensors have been developed by measuring the electrical conductance changes in the GO film upon expose to a humid environment.[23,24]

In the present study we fabricated capacitive-type humidity sensors based on GO and poly(sodium 4-styrenesulfonate) intercalated GO (GO-PSS) composite films, which were used as dielectrics. PSS, which is a hydrophilic and electrically insulating polymer, was used as an intercalant between the individual GO platelets to further enhance the characteristics of water permeation. Freestanding GO and GO-PSS films were prepared by vacuum filtration. Subsequently, gold (Au) electrodes were deposited on both sides of the films by electron beam (e-beam) evaporation, comprising a capacitive-type sensor. The fabricated sensor was then equipped into the charge pumping system, which can produce a voltage output as a response of humidity detection. Therefore, the present device is called a self-powered sensor. The charge pumping system consists of the sensor serially-connected to a reference capacitor, whose operation will be discussed later. The humidity responses of the self-powered sensor were examined in a wide RH range of 0−80%. While both sensors based on GO and GO-PSS responded stably and reversibly to the changes in RH, the GO-PSS sensor showed enhanced sensing responses (~5.6 times higher voltage output and 3 times faster responses in humidity sensing) compared to the GO sensor. We envisioned that the self-powered humidity device presented in this paper is more accessible for electrical measurements and can be applied to devices that harvest electrical energy from the changes in humidity under ambient conditions.

## EXPERIMENTAL SECTION

**Fabrication of the Capacitive-Type Humidity Sensors.** Graphene oxide platelets were synthesized from graphite (Bay Carbon, SP-1) using the modified Hummers method.[25] A solution mixture of graphite powder, sulfuric acid, and potassium permanganate in a beaker was stirred for 6 h at 45 °C. The solution was neutralized by deionized (DI) water and hydrogen peroxide. The brown-colored solution obtained was rinsed 3 times with DI water to completely remove any residual acid and salt in the solution. The GO powders were obtained by filtering the solution using a polytetrafluoroethylene (PTFE) membrane filter (47 mm diameter, 0.2 $\mu$m pore size, Whatman). After the GO powder was prepared, the GO platelets were re-dispersed in DI water with a concentration of 3.0 mg/mL and sonicated for 1 h to make a homogeneous suspension. A GO thin film was formed on the filter by the slow filtration of 16.6 mL of a GO solution over 1 day. To prepare the GO-PSS film, 500 mg PSS (Sigma-Aldrich, MW = 70,000) was dissolved into the 16.6 mL GO solution at a concentration of 3.0 mg/mL and stirred for more than 1 h. A GO-PSS composite film was obtained using the same filtration process used in the fabrication of GO thin films. The thickness of GO and GO-PSS films were measured as ~16 and 27 $\mu$m, respectively. Freestanding GO and GO-PSS films detached from the filter were cut out into a circle with a diameter of 11 mm. The capacitive-type sensors were completed by forming metal electrodes on both sides of the GO and GO-PSS films, as shown in Figure 1a. The present senor has a symmetric structure along the thickness direction, thus no bending deformation of the sensor is generated during the humidity sensing cycles. A 100 nm thick gold film was deposited by e-beam evaporation through a shadow mask with a circular hole of 8 mm. The use of a shadow mask for electrode patterning can exclude the side-effect of the photo-lithographical technique, such as photoresist (PR) residues. Finally, a thin layer of silver paste was coated onto the electrodes to connect an electric wire, followed by drying under ambient conditions. Figure 1a presents a photograph of the fabricated sensor.

**Control of the Relative Humidity.** Precise control of the RH in small controlled-environment chambers can be achieved using two gas

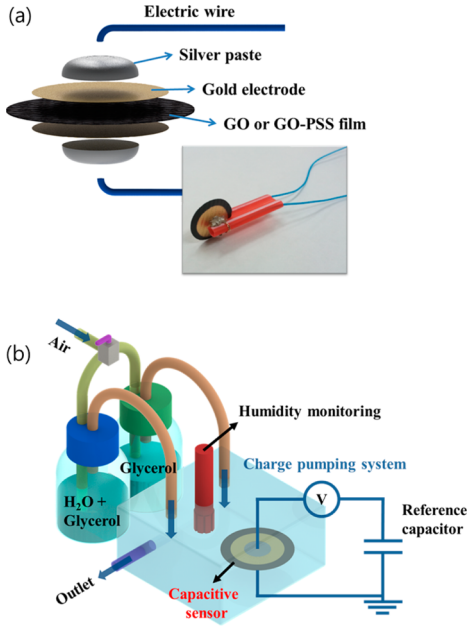


**Figure 1.** (a) Fabrication of the capacitive-type humidity sensor based on the GO and GO-PSS dielectric films. An optical image of the fabricated sensor is shown in the figure. (b) Schematic diagram of the RH controlled-environment chamber and charge pumping system.

washing bottles containing adequate volumes of glycerol−water and glycerol-only solutions.[26] The mixture solution of glycerol and water has several advantages for controlling the RH level in the chamber, such as less corrosive, inexpensive and minimal temperature effects on the equilibrium humidity condition.[26] The relationship between the relative humidity and the volume ratio of the mixed solution is as follows:

$$\frac{V_W}{V_G} = 1.26\left[\frac{1}{3.83\{(-0.189 \times RH + 19.9)^{0.0806} - 1\}} - 1\right] \quad (1)$$

where $V$ is the volume and the subscripts W and G refer to deionized water and glycerol, respectively. The RH denotes the desired percentage relative humidity. As shown in Figure 1b, a gas washing bottle was filled with a mixed solution at a controlled volume ratio and the other bottle was filled with glycerol only. When air flows through the bottle containing solutions of glycerol−water into the chamber, the gas can be humidified by bubbling the mixture solution, adjusting the desired RH level in the chamber. In the same way, the humidity level can be reduced by flowing air through the bottle containing glycerol into the chamber.

**Instruments and Methods.** Scanning electron microscopy (SEM, Hitachi FE-SEM S-4700) was used to observe the cross-sectional structure of the GO and GO-PSS films at an acceleration voltage of 10−15 keV. The interlayer distance of the films were examined quantitatively by X-ray diffraction (XRD, Empyrean series 2) and the chemical binding states and possible interactions between PSS intercalant and GO platelets were characterized by X-ray photoelectron spectroscopy (XPS, Theta Probe AR-XPS system, monochromated Al K$\alpha$, $h\nu$ = 1486.6 eV). Thermogravimetric analysis (TGA) of the films was performed using a TGA Q5000 with 10 °C/min heating rate in nitrogen gas flow. Capacitance measurements of the present sensor were carried out using a broadband dielectric spectrometer (Novocontrol-Concept 80) at a frequency of 50 Hz. The electrical output voltage from the sensor and the humidity in the chamber were monitored using a digital multimeter (Agilent U1252B) and digital humidity logger (Lutron MY-91HT), respectively.


dx.doi.org/10.1021/am501151v | ACS Appl. Mater. Interfaces 2014, 6, 8320−8326

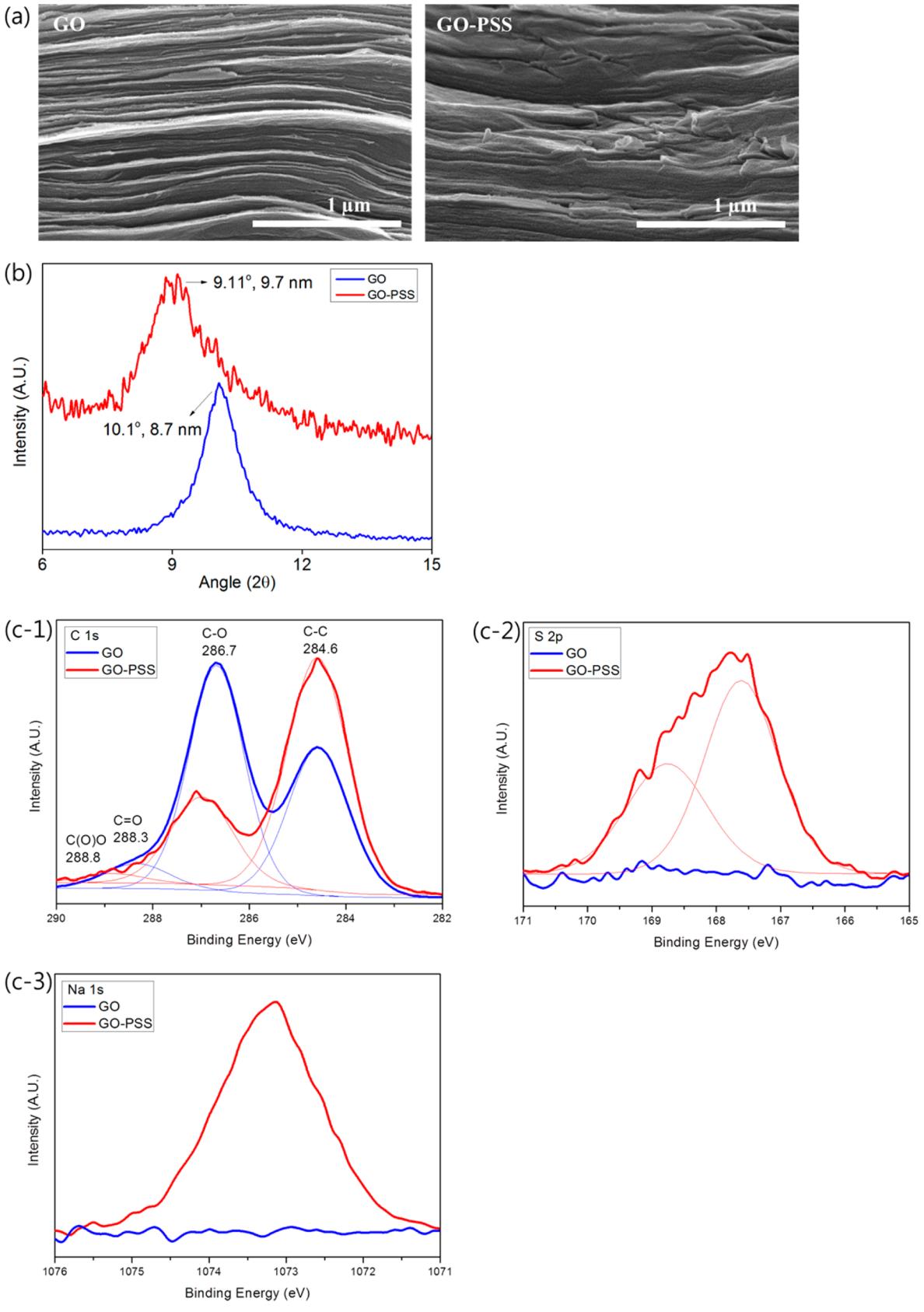


**Figure 2.** Characterization of the GO and GO-PSS films. (a) Cross-sectional SEM images of the films. (b) Determination of the interlayer distance of the GO platelets of the films by XRD. (c) XPS spectrum confirming the presence of PSS and its interaction with GO platelets. The c-1, c-2, and c-3 images show the XPS spectrum of C 1s, S 2p, and Na 1s of the films, respectively.


dx.doi.org/10.1021/am501151v | ACS Appl. Mater. Interfaces 2014, 6, 8320−8326

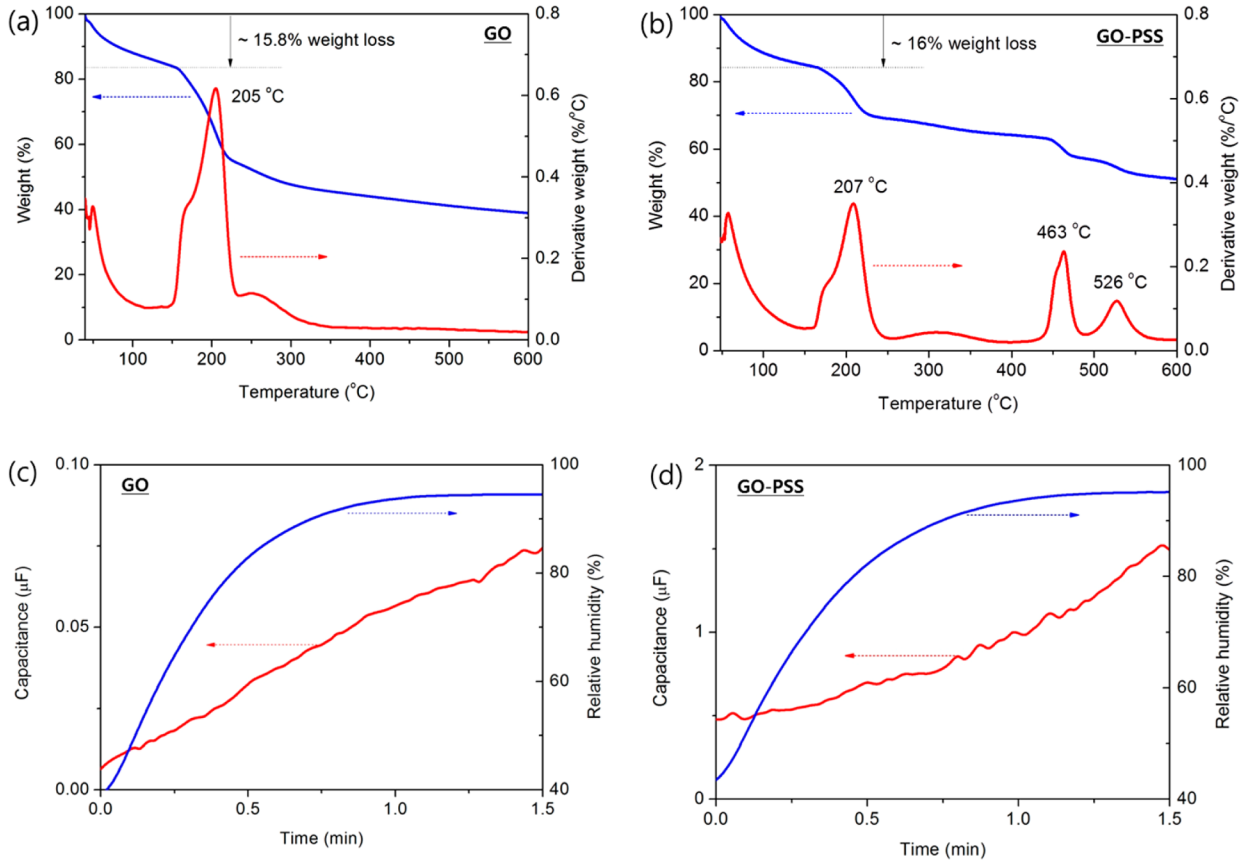


**Figure 3.** Thermal stability and the water absorption capability of the (a) GO and (b) GO-PSS films were examined by TGA. Capacitance change in the sensors based on (c) GO and (d) GO-PSS films with respect to the RH variation.

## RESULTS AND DISCUSSION

The structural features of the laminated GO and GO-PSS films work favorably on the water swelling process by being fast and reversible. Moreover, the intercalation of PSS might enhance the process by extending the interlayer distance of the GO film. The fabricated GO and GO-PSS thin films were first characterized by SEM, as shown in Figure 2a. The cross sectional SEM image of the films revealed uniform and well-stacked GO platelets through almost the entire cross-section of the samples. XRD was performed to determine the interlayer distance of the GO platelets of the film. The XRD (002) peak of the GO film was observed at $2\theta$-10.1°, indicating an interplanar $d$ spacing of 8.7 nm, as shown in Figure 2b. The functionalized oxygen groups on the GO surface and the water molecules trapped in the film result in an increased interlayer distance compared to that of graphite (0.34 nm). The XRD peak shifted to 9.11° in the GO-PSS film, indicating that the interlayer distance is expanded by the presence of the PSS intercalant. XPS provided firm evidence of the PSS intercalation and its interaction with GO platelets. The C 1s XPS spectrum (Figure 2(c-1)) showed a considerable degree of GO oxidation, as reported elsewhere.[28,29] Increased intensity of the non-oxygenated ring C (284.6 eV) was observed in the GO-PSS film, which was assigned to the broad C 1s peak of PSS.[22] The XPS survey scan of the GO-PSS film clearly indicated the presence of PSS. The characteristic peaks for PSS were detected at 167.6 and 168.8 eV (S $2p_{3/2}$ and S $2p_{1/2}$ peaks corresponding to sulfur, Figure 2c-2) and 1073.2 eV (Na 1s peak for sodium, Figure 2c-3) but were entirely absent in the GO film. From the SEM, XRD, and XPS studies, we confirmed that the PSS polymer had been intercalated successfully into the GO films by extending the interlayer distance of the GO film.

The thermal stability and water absorption capability of the GO and GO-PSS films were examined by TGA. Prior to analysis, both specimens were placed in a chamber with a RH being 100% for several hours to allow for swelling water molecules sufficiently, and then loaded immediately into the TGA equipment. The pyrolysis of oxygen containing functional groups in the films induced weight loss at ~200 °C, as shown in Figure 3a and b. In particular, the GO-PSS specimen showed a weight loss at ~500 °C due to thermal decomposition of the PSS polymer. We also observed that the TGA curves at temperatures below 150 °C showed remarkable weight losses of ~15.8% and 16% for the GO and GO-PSS, respectively. Inferred from any thermal decomposition of the specimens were hardly observed at those relatively low temperatures, this considerable weight loss might be assigned to the evaporation of adsorbed water. The water molecules absorbed in the films have a strong interaction with oxygen groups on the GO surface by forming hydrogen bonds.[20] This confined water interaction in the layered and interlocked structure leads to an increase in the dielectric constant across the hydrated GO layers.[21,23] Therefore, a capacitor applied with GO and GO-PSS dielectrics can respond to changes in humidity by the adsorption/desorption of water molecules, in which the response can be monitored by the changes in capacitance. The capacitive-type humidity sensors were simply completed by forming metal electrodes on both sides of the films (detail experimental procedure is reported in the Experimental Section). As shown in Figure 3c and d, the capacitance of


dx.doi.org/10.1021/am501151v | ACS Appl. Mater. Interfaces 2014, 6, 8320−8326

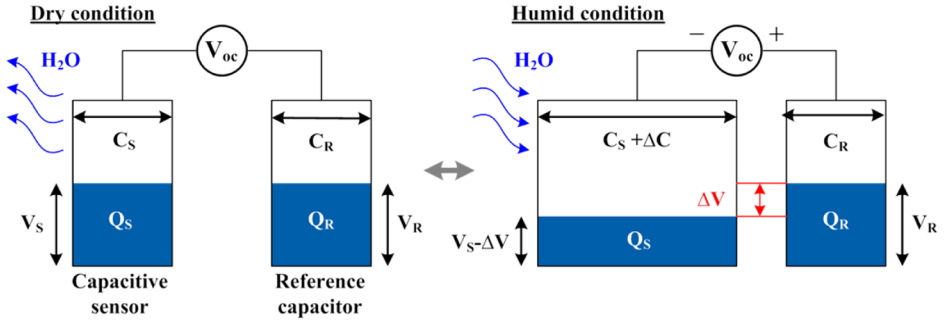


**Figure 4.** Schematic diagram of the operation principle of the charge pumping system.

both sensors increased with increasing RH, however, the GO-PSS sensor showed a superb change in capacitance (~1000 nF) compared to that of the GO film (~70 nF) with on-time. The change in the capacitance of the sensor was dominated mainly by the content of water molecules in the films. Therefore, the PSS intercalant in the GO-PSS film attributes to enhance the characteristics of water permeation by extending the interlayer distance of the GO film. Furthermore, we note that the chemical structure of PSS based on polystyrene with a benzene ring containing sulfonic acid ($SO^{3-}$) and sodium ($Na^{+}$). The sodium ions can be released partially from the sulfonic acid bound covalently to the benzene ring in an electrolyte. When water molecules permeate in a GO-PSS film, a percolated water pathway for conducting ions can be formed. It suggests that the sodium ions move to the electrodes through the pathway, forming an electrical double layer capacitance (EDLC). This capacitance is much larger than the capacitance formed by water only because the ionic strength of sodium ions is greater than the strength of the dipole moment in water. It is noteworthy in this regard that the GO-PSS sensor initially showed ~75 times higher capacitance (480 nF) than the GO film (6.4 nF) at approximately 40% RH. This enhanced charge storage ability (i.e., capacitance) results in an improved change in capacitance of the GO-PSS sensor.

The humidity responsive capacitor (called capacitive sensor) was placed into the charge pumping system shown in Figure 1b, which can produce electrical voltage outputs as a response of humidity sensing. Figure 4 shows a schematic diagram of the operation principle of the charge pumping system. The system consisted of a capacitive sensor connected serially to a capacitor (called reference capacitor), which is commercially available and insensitive to changes in humidity. After exposing the capacitive sensor to a humid environment, the capacitance ($C_s$) increased, and the voltage ($V_s$) decreased simultaneously based on the relationship between the voltage supplied to a capacitor and the charge stored (i.e., $Q = CV$). Therefore, an electrical potential difference ($\Delta V$) is generated between the two capacitors, which can be inferred by measuring the open-circuit voltage ($V_{oc}$). When the charge pumping system is connected to an external electrical load, the potential difference drives electrons in the external circuit so that electrical current and power can be delivered. Therefore, the present system also demonstrates a possible technology that scavenges electrical energy from the changes in humidity under ambient conditions.

The performance of the self-powered humidity sensor was examined by measuring an open-circuit voltage over a wide RH range from 0% to 80% with increasing 20%. The output voltage generated from the both GO and GO-PSS based sensors varies reversibly with respect to the RH variations, the GO-PSS sensor responds more quickly to changes in humidity rather than the GO sensor, which was evidenced by comparing the slope of the output voltage curves in Figure 5a and b. The response and recovery times, as the time required to reach 90% of the peak voltage,[27] were measured as ~150 and ~50 for GO and GO-PSS sensors, respectively (See Figure S1 in Supporting Information). The GO-PSS sensor was able to fully follow the humidity modulation, showing almost 3 times fast in response and recovery time.

The hysteresis loops of the voltage generated from the GO and GO-PSS sensors are shown in Supporting Information Figure S2a and S2b, respectively. While the sensor based on GO film was too slow to follow the humidity modulation (see Figure 5a), inducing large hysteresis loops; the GO-PSS sensor shows small hysteresis in generating voltage. In particular, the hysteresis loops in GO-PSS sensor is mainly caused by the discharge of electrons stored in the sensor. GO and GO-PSS films used as dielectrics are not a perfect insulator but having electrically conductive path in the films. Oxygen functional groups on the GO surface tend to cluster leaving large, percolating regions of a graphene sheet pristine.[17] Therefore, the GO-PSS sensor might discharge electrons charged in the sensor through the conduction path, causing a voltage drop as shown in Supporting Information Figure S2b.

Figure 5c shows the maximum output voltage as a function of the RH level. The present self-powered humidity sensors showed a linear relationship between the output voltage and RH level. As shown in the figure, the GO-PSS sensor showed remarkable enhancement of the output voltage signals. A linear-fit revealed the GO-PSS sensor to have a ~5.6 times higher voltage response than that of the GO sensor over the RH range, 0 to 80%. The improvements in humidity sensing were attributed to the improved water permeation characteristics with the extended interlayer distance and the large charge store capability in the GO-PSS film.

## CONCLUSIONS

The self-powered humidity sensors were fabricated using the GO and the PSS-intercalated GO composite films. The PSS polymer was used as an intercalant between the individual GO platelets to enhance the characteristics of water permeation and to increase the capacitance of the film. The successful intercalation of PSS was confirmed using a range of techniques, such as SEM, XRD and XPS analysis. The capacitive-type humidity sensor fabricated by forming metal electrodes on the film was equipped into the charge pumping system, which can produce voltage outputs as a response to humidity sensing. The performance of the self-powered sensor, such as capacitance change, voltage generation and response time, were evaluated

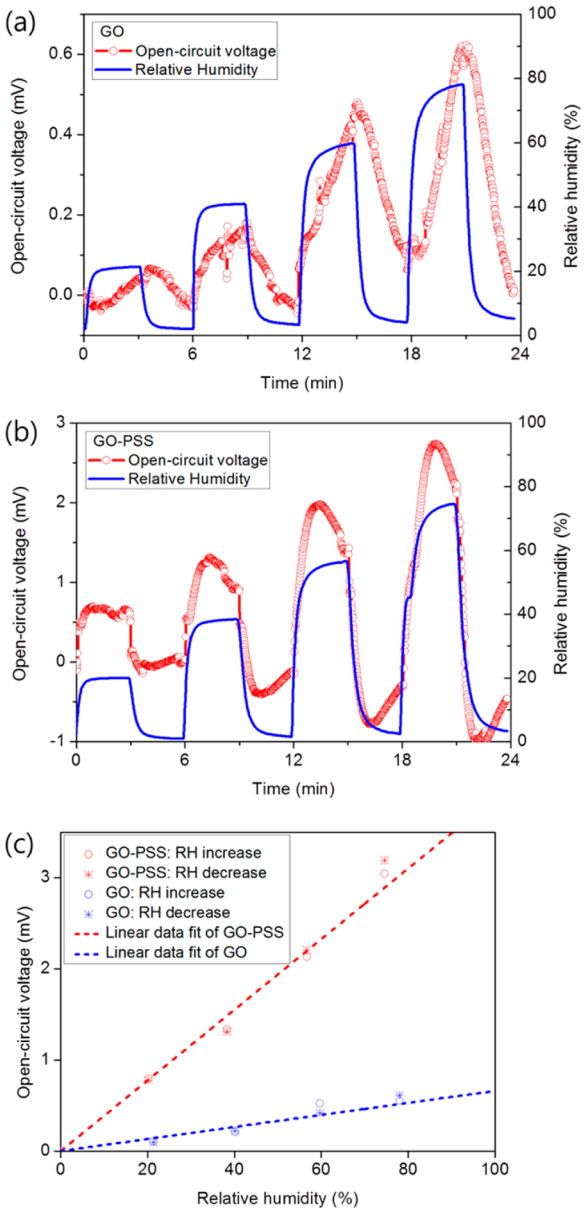


**Figure 5.** Performance evaluation of the self-powered humidity sensor. (a, b) Voltage outputs of the GO and GO-PSS sensors were investigated over the RH range, 0−80%, respectively. (c) Maximum output voltage as a function of the RH level is plotted in the figure.

quantitatively. The sensor based on the GO-PSS film showed remarkable enhancement of the sensing performance compared to that of the GO sensor. The GO-PSS sensor showed rapid responses to changes in humidity and the voltage response was ~5.6 times higher over a wide RH range (0−80%) than that of the GO sensor. Improved water permeation characteristics by extending the interlayer distance and the large charge store capability in GO-PSS films were responsible for the improvements in humidity sensing. Finally, the present self-powered device can generate a voltage output upon exposure to humid environments, suggesting a possible device that scavenges electrical energy from the changes in humidity under ambient conditions.

## ■ ASSOCIATED CONTENT

### Supporting Information

Response and recovery times of the present sensors and hysteresis loops of the voltage generated from the GO and GO-PSS sensors. This material is available free of charge via the Internet at http://pubs.acs.org.

## ■ AUTHOR INFORMATION

### Corresponding Authors

*E-mail: tjkang@pusan.ac.kr). Tel.: +82-51-510-7411.
*E-mail: yongkim@snu.ac.kr. Tel.: +82-2-880-7385.

### Notes

The authors declare no competing financial interest.

## ■ ACKNOWLEDGMENTS

This study was supported by the National Research Foundation of Korea (Grants 2009-0083512, 2009-0078659, and 2011-0024818), and supported by Defense Acquisition Program Administration and Agency for Defense Development under Contract UD100048JD, the Civil & Military Technology Cooperation Program through the National Research Foundation of Korea (NRF) funded by the Ministry of Science, ICT & Future Planning (No. 2013M3C1A9055407), "Development of Multi-Physics based Micro Manufacturing (MP-M2) Technologies for Biomedical Projects" International Collaborative R&D Program project of ministry of knowledge economy, and "Development of Nano-level Surface Reformation Process and an Equipment using Ultrasonic Vibration" of the Ministry of Trade, Industry and Energy (MOTIE). The authors also acknowledge support from the Institute of Advanced Aerospace Technology at Seoul National University.

## ■ REFERENCES

(1) Sakai, Y.; Sadaoka, Y.; Matsuguchi, M. Humidity Sensors Based on Polymer Thin Films. *Sens. Actuators, B* **1996**, *35*, 85−90.
(2) Gu, L.; Huang, Q.-A.; Qin, M. A Novel Capacitive-type Humidity Sensor using CMOS Fabrication Technology. *Sens. Actuators, B* **2004**, *99*, 491−498.
(3) Matsuguchi, M.; Umeda, S.; Sadaoka, Y.; Sakai, Y. Characterization of Polymers for a Capacitive-Type Humidity Sensor Based on Water Sorption Behavior. *Sens. Actuators, B* **1998**, *49*, 179−185.
(4) Huang, H.; Sun, A.; Chu, C.; Li, Y.; Xu, G. Electrical and Humidity Sensing Properties of Graphene and Polystyrene Sulfonic Sodium Bilayer Thin Film. *Integr. Ferroelectr.* **2013**, *144*, 127−134.
(5) Huang, X.; Sun, Y.; Wang, L.; Meng, F.; Liu, J. Carboxylation Multi-walled Carbon Nanotubes Modified with $LiClO_4$ for Water Vapour Detection. *Nanotechnology* **2004**, *15*, 1284−1288.
(6) Su, P.-G.; Wang, C.-S. Novel Flexible Resistive-type Humidity Sensor. *Sens. Actuators, B* **2007**, *123*, 1071−1076.
(7) Yoo, K.-P.; Lim, L.-T.; Min, N.-K.; Lee, M. J.; Lee, C. J.; Park, C.-W. Novel Resistive-type Humidity Sensor Based on Multiwall Carbon Nanotube/Polyimide Composite Films. *Sens. Actuators, B* **2010**, *145*, 120−125.
(8) Bariain, C.; Matías, I. R.; Arregui, F. J.; Lopez-Amo, M. Optical Fiber Humidity Sensor Based on a Tapered Fiber Coated with Agarose Gel. *Sens. Actuators, B* **2000**, *69*, 127−131.
(9) Muto, S.; Suzuki, O.; Amano, T.; Morisawa, M. A Plastic Optical Fibre Sensor for Real-Time Humidity Monitoring. *Meas. Sci. Technol.* **2003**, *14*, 746−750.
(10) Ahmad, M. M.; Makhlouf, S. A.; Khalil, K. M. S. Dielectric Behavior and AC Conductivity Study of $NiO/Al_2O_3$ Nanocomposites in Humid Atmosphere. *J. Appl. Phys.* **2006**, *100*, No. 094323.
(11) Kuang, Q.; Lao, C.; Wang, Z. L.; Xie, Z.; Zheng, L. High-Sensitivity Humidity Sensor Based on a Single $SnO_2$ Nanowire. *J. Am. Chem. Soc.* **2007**, *129*, 6070−6071.

(12) Zhang, Y.; Yu, K.; Jiang, D.; Zhu, Z.; Geng, H.; Luo, L. Zinc Oxide Nanorod and Nanowire for Humidity Sensor. *Appl. Surf. Sci.* **2005**, *242*, 212−217.
(13) Buchsteiner, A.; Lerf, A.; Pieper, J. Water Dynamics in Graphite Oxide Investigated with Neutron Scattering. *J. Phys. Chem. B* **2006**, *110*, 22328−22338.
(14) Cerveny, S.; Barroso-Bujans, F.; Alegría, A. n.; Colmenero, J. Dynamics of Water Intercalated in Graphite Oxide. *J. Phys. Chem. C* **2010**, *114*, 2604−2612.
(15) Lerf, A.; Buchsteiner, A.; Pieper, J.; Schöttl, S.; Dekany, I.; Szabo, T.; Boehm, H. Hydration Behavior and Dynamics of Water Molecules in Graphite Oxide. *J. Phys. Chem. Solids* **2006**, *67*, 1106−1110.
(16) Dreyer, D. R.; Park, S.; Bielawski, C. W.; Ruoff, R. S. The Chemistry of Graphene Oxide. *Chem. Soc. Rev.* **2010**, *39*, 228−240.
(17) Nair, R.; Wu, H.; Jayaram, P.; Grigorieva, I.; Geim, A. Unimpeded Permeation of Water Through Helium-Leak-Tight Graphene-Based Membranes. *Science* **2012**, *335*, 442−444.
(18) Yao, Y.; Chen, X.; Guo, H.; Wu, Z. Graphene Oxide Thin Film Coated Quartz Crystal Microbalance for Humidity Detection. *Appl. Surf. Sci.* **2011**, *257*, 7778−7782.
(19) Yao, Y.; Chen, X.; Guo, H.; Wu, Z.; Li, X. Humidity Sensing Behaviors of Graphene Oxide-silicon Bi-layer Flexible Structure. *Sens. Actuators, B* **2012**, *161*, 1053−1058.
(20) Wang, D.-W.; Du, A.; Taran, E.; Lu, G. Q. M.; Gentle, I. R. A Water-Dielectric Capacitor Using Hydrated Graphene Oxide Film. *J. Mater. Chem.* **2012**, *22*, 21085−21091.
(21) Compton, O. C.; Jain, B.; Dikin, D. A.; Abouimrane, A.; Amine, K.; Nguyen, S. T. Chemically Active Reduced Graphene Oxide with Tunable C/O Ratios. *ACS Nano* **2011**, *5*, 4380−4391.
(22) Jeong, H.-K.; Jin, M. H.; An, K. H.; Lee, Y. H. Structural Stability and Variable Dielectric Constant in Poly Sodium 4-styrensulfonate Intercalated Graphite Oxide. *J. Phys. Chem. C* **2009**, *113*, 13060−13064.
(23) Guo, L.; Jiang, H.-B.; Shao, R.-Q.; Zhang, Y.-L.; Xie, S.-Y.; Wang, J.-N.; Li, X.-B.; Jiang, F.; Chen, Q.-D.; Zhang, T. Two-Beam-Laser Interference Mediated Reduction, Patterning and Nanostructuring of Graphene Oxide for the Production of a Flexible Humidity Sensing Device. *Carbon* **2012**, *50*, 1667−1673.
(24) Zhao, C.-L.; Qin, M.; Huang, Q.-A. Humidity Sensing Properties of the Sensor Based on Graphene Oxide Films with Different Dispersion Concentrations. *IEEE Sens. Proc.* **2011**, 129−132.
(25) Marcano, D. C.; Kosynkin, D. V.; Berlin, J. M.; Sinitskii, A.; Sun, Z.; Slesarev, A.; Alemany, L. B.; Lu, W.; Tour, J. M. Improved Synthesis of Graphene Oxide. *ACS Nano* **2010**, *4*, 4806−4814.
(26) Forney, C. F.; Brandl, D. G. Control of Humidity in Small Controlled-environment Chambers using Glycerol−Water Solutions. *HortTechnology* **1992**, *2*, 52−54.
(27) Mogera, U.; Sagade, A. A.; George, S. J.; Kulkarni, G. U. Ultrafast Response Humidity Sensor using Supramolecular Nanofibre and Its Application in Monitoring Breath Humidity and Flow. *Sci. Rep.* **2014**, *4*, 4103.